As compared with the existing techniques for calibration of bolometer mounts, the methods proposed herein may appear unduly complex, at least in terms of operator effort. On the other hand, it must be recognized that the coupler–mount assembly is a two-port device, and to the author, at least, this increase in complexity appears unavoidable.

ACKNOWLEDGMENT

The author wishes to thank B. C. Yates and L. B. Elwell for their constructive suggestions in the preparation of this paper.

REFERENCES

[1] R. F. Pramann, "Automated characterization of bolometric and electrothermic mounts," *IEEE Trans. Instrum. Meas. (1970 Conf. on Precision Electromagnetic Measurements)*, vol. IM-19, pp. 239–245, Nov. 1970.
[2] F. R. Hume, F. K. Koide, and D. J. Dederich, "Practical and precise means of microwave power meter calibration transfer," *IEEE Trans. Instrum. Meas. (1972 Conf. on Precision Electromagnetic Measurements)*, vol. IM-21, pp. 457–466, Nov. 1972.
[3] E. L. Komarek and P. V. Tryon, "An application of the power equation concept and automation techniques to precision bolometer unit calibration," *IEEE Trans. Microwave Theory Tech. (Part II of Two Parts: 1974 Symp. Issue)*, vol. MTT-22, pp. 1260–1267, Dec. 1974.
[4] G. F. Engen, "Amplitude stabilization of a microwave signal source," *IRE Trans. Microwave Theory Tech.*, vol. MTT-6, pp. 202–206, Apr. 1958.
[5] ——, "Calibration technique for automated network analyzers with application to adapter evaluation," *IEEE Trans. Microwave Theory Tech. (Part II of Two Parts: 1974 Symp. Issue)*, vol. MTT-22, pp. 1255–1260, Dec. 1974.
[6] ——, "Power equations: A new concept in the description and evaluation of microwave systems," *IEEE Trans. Instrum. Meas.*, vol. IM-20, pp. 49–57, Feb. 1971.
[7] I. Kasa, "Closed-form mathematical solutions to some network analyzer calibration equations," *IEEE Trans. Instrum. Meas. (1974 Conf. on Precision Electromagnetic Measurements)*, vol. IM-23, pp. 399–402, Dec. 1974.
[8] G. F. Engen, "Comments on 'Practical analysis of reflectometers and power equation concepts'," *IEEE Trans. Instrum. Meas.* (Short Papers), vol. IM-23, pp. 104–105, Mar. 1974.
[9] ——, "Theory of UHF and microwave measurements using the power equation concept," Nat. Bur. Stand., Boulder, Colo., Tech. Note 637.

Three-Dimensional Transmission-Line Matrix Computer Analysis of Microstrip Resonators

SINA AKHTARZAD AND PETER B. JOHNS

Abstract—**A wide range of microwave resonators are analyzed using the same three-dimensional transmission-line-matrix (TLM) computer program. The paper demonstrates the ease of application, versatility, and accuracy of the TLM method. The results presented include the dispersion characteristics of microstrip on dielectric and magnetic substrates and an example of a microstrip discontinuity. The surface-mode phenomenon of microstrip is also investigated.**

I. INTRODUCTION

THE SOLUTION of large microwave integrated circuit (MIC) subassemblies presents a major problem to any numerical method. However, it would seem that the first step should involve a numerical routine of a very general nature for simple discontinuities in three-dimensional structures. There are many articles giving design data for single microstrip ([1]–[5], for example), pairs of coupled strips ([6]–[9], for example), and coplanar waveguides ([10] and [11]). Discontinuities which can occur in simple configurations such as abruptly ended strip conductor [12]–[14] and strip-width variation [12] have also been reported. Some of these publications use methods based on static approximations and all of them tend to use fairly specialized techniques and programs. Thus the design engineer does not have a universal and general program for solving a wide range of problems. The transmission-line matrix (TLM) [15], [16] method of numerical analysis in the form of a very general and short program fulfills this requirement.

The purpose of this paper is twofold: firstly, to review the general state of the art of the TLM method as far as the modeling of three-dimensional cavities is concerned; Secondly, to demonstrate the accuracy and the versatility

Manuscript received April 14, 1975; revised July 28, 1975. This work was supported by the United Kingdom Ministry of Defence under Contract AT/2024/037/CVD.

S. Akhtarzad is with the Department of Electrical and Electronic Engineering, University of Nottingham, University Park, Nottingham, NG7, 2RD, England.
P. B. Johns is with the Department of Electrical and Electronic Engineering, University of Nottingham, University Park, Nottingham, NG7, 2RD, England, on leave at the Department of Electrical Engineering, University of Manitoba, Winnipeg, Man., Canada.

of this method in the form of a computer program by means of a few typical microstrip cavity examples. It should be noted that all the examples presented in this paper have been analyzed strictly in three dimensions using various lengths of cavity to obtain the dispersion curves.

II. A BRIEF OUTLINE OF THE TLM METHOD

The TLM numerical method in two dimensions [17] has been extensively explored in various papers where it has been used to solve general two-dimensional loss-free [18] and lossy inhomogeneous [15] field problems. In two dimensions the method is based on a network of shunt nodes connected together to represent a propagating space. However, the method has now been extended to use shunt nodes [Fig. 1(a)] in conjunction with series nodes [15] [Fig. 1(b)] to represent a true three-dimensional [15] space so that each three-dimensional node consists of three shunt and three series nodes. The three shunt nodes represent the E-field, and the three series nodes represent the H-field in the three coordinate directions as shown in Fig. 1(c) (note that in Fig. 1(c) single lines are used to represent a pair of lines). To accommodate discontinuities such as metallic boundaries and slabs of dielectric or magnetic material, open-circuited and short-circuited lengths of lines (stubs) of variable, normalized characteristic admittance Y_0 and Z_0 are added to shunt and series nodes, respectively. By varying the values of Y_0 and Z_0, the values of permittivity (ϵ_r) and permeability (μ_r), respectively, at the node, can be fixed to any desired value. The three-dimensional node is further equipped with stubs of infinite length and normalized characteristic admittance G_0 at the shunt nodes to facilitate any dielectric losses which may be required. The three-dimensional geometry of a problem is set up by connecting many such three-dimensional nodes together.

Let us now examine the three-dimensional node of Fig. 1(c) more closely. In [15] it is shown that if the voltage (v) between the lines represents the E-field, and the current (I) in the lines represents the H-field, then the field equations satisfied by a three-dimensional node correspond to the set of Maxwell's equations as follows:

$$\frac{\partial H_z}{\partial y} - \frac{\partial H_y}{\partial z} = \epsilon_0\epsilon_r \frac{\partial E_x}{\partial t} + \sigma E_x \tag{1}$$

$$\frac{\partial H_x}{\partial z} - \frac{\partial H_z}{\partial x} = \epsilon_0\epsilon_r \frac{\partial E_y}{\partial t} + \sigma E_y \tag{2}$$

$$\frac{\partial H_y}{\partial x} - \frac{\partial H_x}{\partial y} = \epsilon_0\epsilon_r \frac{\partial E_z}{\partial t} + \sigma E_z \tag{3}$$

$$\frac{\partial E_z}{\partial y} - \frac{\partial E_y}{\partial z} = -\mu_0\mu_r \frac{\partial H_x}{\partial t} \tag{4}$$

$$\frac{\partial E_x}{\partial z} - \frac{\partial E_z}{\partial x} = -\mu_0\mu_r \frac{\partial H_y}{\partial t} \tag{5}$$

$$\frac{\partial E_y}{\partial x} - \frac{\partial E_x}{\partial y} = -\mu_0\mu_r \frac{\partial H_z}{\partial t}. \tag{6}$$

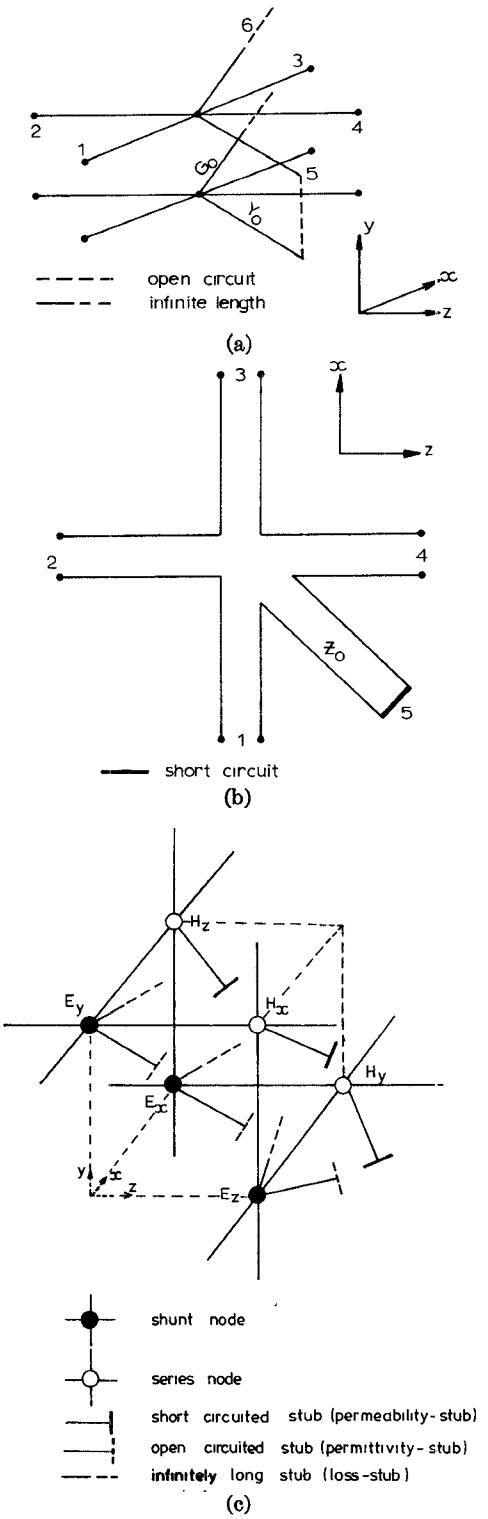

Fig. 1. (a) Shunt-connected node with permittivity and loss stubs. (b) Series-connected node with permeability stub. (c) Schematic diagram of a three-dimensional node including the permittivity, permeability, and loss stubs (two-dimensional node separation and stub length = $\Delta l/2$). Note that the dotted lines making up the corners of the cube are guide lines and do not represent transmission lines or stubs.

In these equations, the following equivalences apply:

$E_x \equiv$ the common voltage at shunt node E_x.

$E_y \equiv$ the common voltage at shunt node E_y.

$E_z \equiv$ the common voltage at shunt node E_z.

$H_x \equiv$ the common current at series node H_x

$H_y \equiv$ the common current at series node H_y

$H_z \equiv$ the common current at series node H_z

$\epsilon_0 \equiv C$ (the capacitance per unit length of lines)

$\epsilon_r \equiv 2(1 + Y_0/4)$

$\mu_0 \equiv L$ (the inductance per unit length of lines)

$\mu_r \equiv 2(1 + Z_0/4)$

$$\sigma \equiv G_0/((L/C)^{1/2} \cdot \Delta l) \tag{7}$$

where $\Delta l/2$ is the spacing between the individual two-dimensional elementary nodes.

Therefore, it can be seen that the six components of the electromagnetic (EM) field at a three-dimensional node are readily available at the corners of the three-dimensional node cube and are analogous to common voltages or common currents at the shunt or series nodes. Furthermore, it is noticed that permeability (μ_r), or permittivity (ϵ_r) and conductivity (σ) of part of the space represented by the three-dimensional node may be made variable simply by adjusting the normalized characteristic values of stubs Z_0, Y_0, and G_0, respectively. The three-dimensional node represents a cube volume of space of $\Delta l/2$ long in each direction. Interconnection of many such three-dimensional nodes makes it possible to describe any complicated inhomogeneous media. The TLM method is then concerned with obtaining the impulse response of such network representing the media. The numerical routine is therefore based upon the voltage impulse scattering matrix of the individual two-dimensional nodes forming the three-dimensional node. The voltage scattering matrix for the shunt node [15] is

$$\frac{2}{Y}\begin{bmatrix} 1 & 1 & 1 & 1 & Y_0 \\ 1 & 1 & 1 & 1 & Y_0 \\ 1 & 1 & 1 & 1 & Y_0 \\ 1 & 1 & 1 & 1 & Y_0 \\ 1 & 1 & 1 & 1 & Y_0 \end{bmatrix} - \mathcal{I} \tag{8}$$

where

$$Y = 4 + Y_0 + G_0. \tag{9}$$

Similarly, the voltage scattering matrix for the series node [15] is given by

$$\frac{2}{Z}\begin{bmatrix} -1 & 1 & 1 & -1 & -1 \\ 1 & -1 & -1 & 1 & 1 \\ 1 & -1 & -1 & 1 & 1 \\ -1 & 1 & 1 & -1 & -1 \\ -Z_0 & Z_0 & Z_0 & -Z_0 & -Z_0 \end{bmatrix} + \mathcal{I} \tag{10}$$

where

$$Z = 4 + Z_0. \tag{11}$$

In these equations $\mathcal{I}$ is the unit matrix.

Conducting boundaries and strips of a problem are simulated in the model by means of short-circuiting the individual shunt nodes in the plane of the boundary or strip. The boundaries may be made lossy by using imperfect reflection coefficients [19]. Open-circuit planes of symmetry may be utilized to make use of the onefold, twofold, or threefold symmetry of a particular structure. This would, of course, lower both memory stores and run-time requirements of a program considerably. An open-circuit plane may be simulated by means of open-circuiting the individual series nodes lying on the plane.

For the purpose of the analysis, any of the six EM field components is excited by introducing impulses at various points in the network model. The initial sign and amplitude of a field component can be fixed using appropriate initial impulse values. These impulses travel along the ideal TEM lines and are scattered at the individual two-dimensional nodes according to (8)–(11). In this way, the time-domain propagation of all six EM field components is obtained simultaneously. A solution for any (or all) of the field components is available anywhere within the geometry of the problem. The output consists of a stream of impulse amplitudes corresponding to the output impulse function for the particular field component under consideration. Finally, the Fourier transform of this function is taken to yield the response to an excitation varying sinusoidally with time.

A general-purpose computer program based on the preceding analysis has been written. This program is highly versatile and all the information relating to a three-dimensional resonator, such as conducting boundaries, strip patterns, permeability, and permittivity at different points and also losses, is simply fed into the computer as data. The three-dimensional program is an extension of the two-dimensional TLM program [20] and has been written in only 110 lines of Fortran *including* three short subroutine programs. This program is used to obtain results for all the following examples in this paper. These specific examples have been chosen for the sole purpose of comparison with other results available.

III. MICROSTRIP CAVITIES

The general TLM program has been used to find the resonant frequencies of three-dimensional cavities containing microstrip. The first microstrip cavity checked on the computer corresponded to the structure of Fig. 2. In the TLM method the resonant frequencies of cavities with various lengths (L) are used to plot frequency in gigahertz versus phase constant (β) curve. The TLM result is compared with Mittra and Itoh [3] and Hornsby and Gopinath [4] in Fig. 2. The quasi-TEM solution for open microstrip line based on Wheeler's curves [1] is also shown for comparison. The frequency versus phase constant curve for the quasi-TEM analysis shows no dispersion. This is due to the fact that the dispersion effect is neglected in

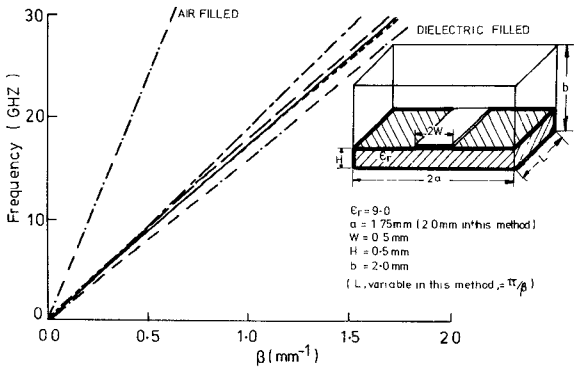

Fig. 2. Dispersion diagram of enclosed microstrip line ($a/\Delta l = 4$). ——, TLM method; – – –, Mittra and Itoh; - - - - -, Hornsby and Gopinath; – · –, quasi-TEM (open microstrip).

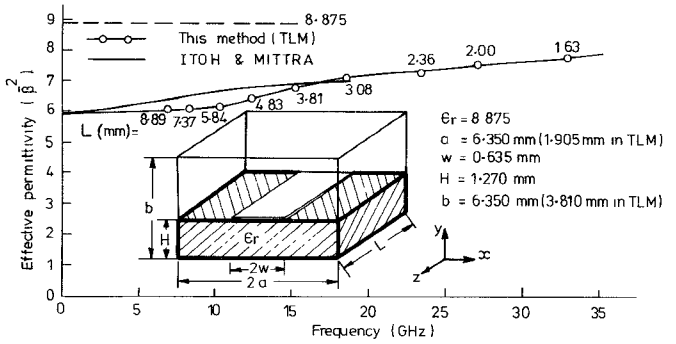

Fig. 3. Effective dielectric constant versus frequency ($2a/\Delta l = 15, 21$).

such an analysis. The curves of Fig. 2 demonstrate the high accuracy of the results obtained by this method, even though a very small number of nodes (see the figure) have been used to describe the geometry of the problem.

Longitudinal field components effect a phase velocity decrease with increasing frequency. $\bar{\beta} = \beta/\beta_0 = \epsilon_{\text{eff}}^{1/2}$ describes the frequency-dependent behavior of effective permittivity. Fig. 3 shows the frequency dependence of ϵ_{eff} for a microstrip cavity shown in the same figure. In Fig. 3, the effective permittivity versus frequency curve obtained by the TLM method for various lengths of cavity (L) is compared with that given by Itoh and Mittra [21]. A full description of the method used in [21] is given in [13]. Note that the method used in [13] by the author, Itoh, differs from that given in [3] by Mittra and Itoh.

IV. MICROSTRIP LINE ON MAGNETIC SUBSTRATE

The method is used to calculate the dispersion relationship for a microstrip line on an isotropic magnetic substrate. The example is given for a relative permeability of $\mu_r = 0.8$ which is within a practical range of permeabilities for substrates biased along the direction of propagation [22]. The results are shown in Fig. 4 and are compared with the result obtained by Pucel and Massé [22] assuming TEM propagation. As expected, the results agree for low frequencies, and the discrepancy between the TEM assumption and the true dispersive result obtained by

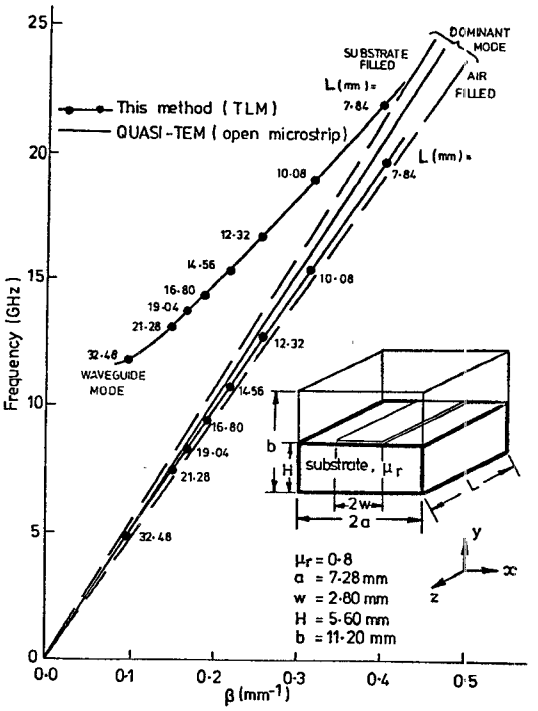

Fig. 4. Dispersion diagram of enclosed microstrip line on an isotropic magnetic substrate ($2a/\Delta l = 13$).

the TLM method becomes important only at high frequencies.

Pucel and Massé have derived a duality relationship between magnetic and dielectric substrates, again assuming TEM propagation. This relationship allows calculation of the effective permeability μ_{eff} in terms of effective permittivity ϵ_{eff} by the formula [22]

$$\mu_{\text{eff}}(W/H,\mu) = \frac{1}{\epsilon_{\text{eff}}(W/H,\mu^{-1})}.$$

In [23], using the TLM method, it is shown how the product $\mu_{\text{eff}} \cdot \epsilon_{\text{eff}}$ varies with frequency for substrates with $\mu_r = 0.8$ ($\epsilon_r = 1$) and $\epsilon_r = 1.25$ ($\mu_r = 1$). The results show that at low frequencies the TEM approximation applies since the product is near unity. At high frequencies μ_{eff} tends to unity and the product then asymptotes to ϵ_{eff}. The near-linear variation of ϵ_{eff} with frequency suggests that the approximate method for calculating μ_{eff} used by Pucel and Massé [24] yields good results.

In Fig. 4 the dispersion curve obtained by this method for the first waveguide mode of the same structure is also shown. It must be noted that since the TLM method operates in the time domain, the output impulse function also contains the information about the higher order modes. Therefore in Fig. 4, each pair of resonant frequencies corresponding to the same β (or L) have been obtained in one run of the program.

V. MICROSTRIP DISCONTINUITIES

The versatility of both the TLM method and the TLM program is further illustrated here by calculating the resonant frequencies of cavities containing microstrip with an abrupt change in width.

Fig. 5 shows the geometry of a dielectric-loaded cavity with a microstrip line. The width of the center line is nonuniform with an abrupt change. Some representative numerical results of this geometry are shown in Fig. 6. The TLM results are compared with a curve calculated by TEM analysis with a capacitive discontinuity given by Farrar and Adams [12]. Farrar and Adams obtain their results using a matrix method which is based on the quasi-static approximation. From Fig. 6 it is apparent that the relative values of frequency for short lengths ($2L$) of the cavity are considerably lower than those computed by the quasi-static approximations. This is partly due to the lack of dispersion in the continuous sections when employing TEM analysis. The discrepancy is due to the fact that there is a fringing field effect between the discontinuity edges and the front conducting plane of the cavity (Fig. 5) in the TLM results. For a short length of L in Fig. 5, the fringing capacitance will have an effect comparable with that of the discontinuity and hence the larger differences at this region.

The dispersive curve for a uniform line with $W = W_0 =$ 1.75 mm is also shown in Fig. 6. This shows that the dispersion due to the line itself is far more important than the dispersion due to the discontinuity. Hence a solution based on the quasi-TEM analysis of the complete structure would be misleading.

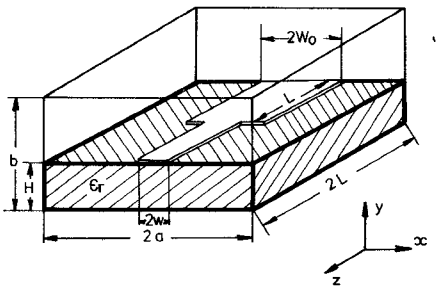

Fig. 5. Microstrip cavity with an abrupt change in linewidth.

VI. INVESTIGATION OF THE LOW-LOSS MICROSTRIP MODE

It is well known that the dominant mode of propagation in the inhomogeneous structures is basically the quasi-TEM mode with a dc cutoff frequency. However, in [5], using the finite-element method of numerical analysis [25], Daly has predicted the existence of a second type of mode also with a dc cutoff frequency. The particular mode has been referred to as surface wave due to the heavy concentration of all field components near the air–dielectric interface. The longitudinal fields for this mode decay rapidly away from the interface as in surface waveguides [26], [27]. Daly argues that due to the smallness of the electric field at the conductor, for a given surface resistivity, the losses in the surface wave would be very much smaller than for the quasi-TEM waves. The same general argument would also hold if the dielectric were lossy. The dispersion in the proposed surface mode was also predicted to be negligible compared to that for the TEM mode.

These desirable properties highlight the importance of investigating the existence and properties of this mode and an attempt has been made to do this using the TLM method. Thus the structure of the example used by Daly was reproduced in the computer in order to compare his results with the TLM results. The geometry of the structure is shown in Fig. 7. For the purpose of representation, in Fig. 7 results are compared for frequency versus phase

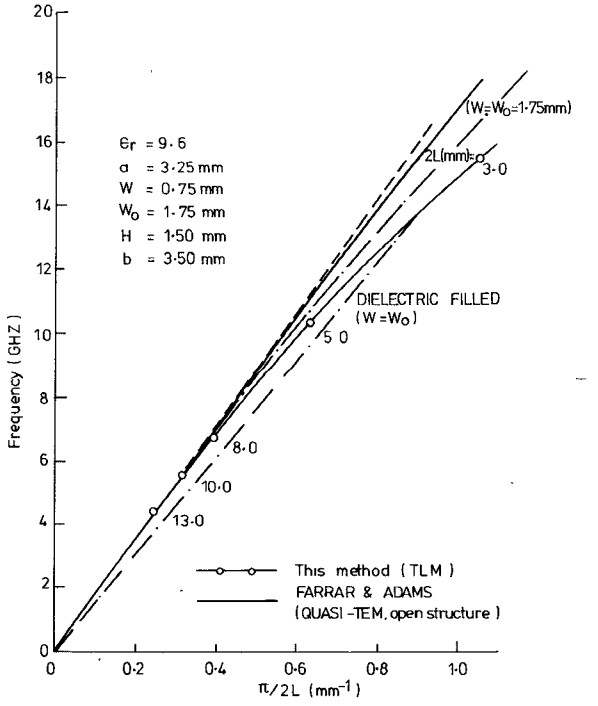

Fig. 6. Dispersion diagram for structure of Fig. 5 ($2a/\Delta l = 13$).

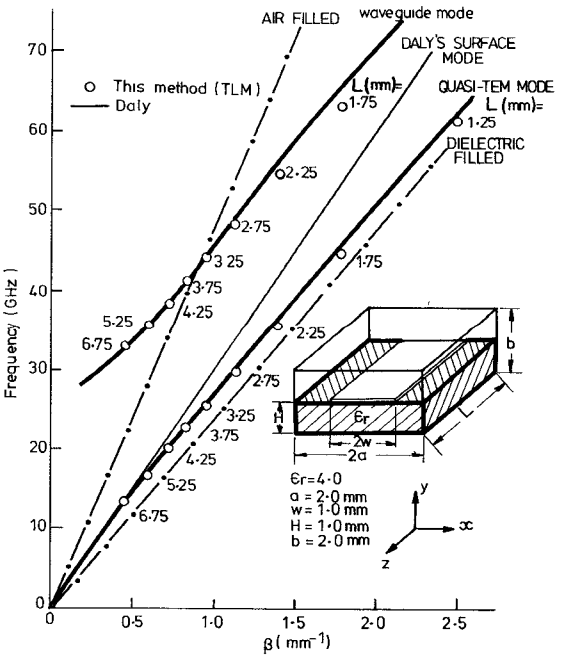

Fig. 7. Dispersion diagram of enclosed microstrip line ($a/\Delta l = 8$).

constant rather than frequency versus effective permittivity [5]. Considerable care was taken to try to excite the surface mode as suggested by Daly, and the cavity was even excited with Daly's field values as given in [5]. However, there was no resonant frequency corresponding to this mode, even though higher order waveguide modes are readily detected. (Note that in [15], the same microstrip structure, but without the strip, was used to obtain accurate surface-waveguide-mode results.)

Figs. 8 and 9 show a typical E_y-field amplitude versus normalized frequency $\Delta l/\lambda$ for the cavity of Fig. 7, with $L = 3.75$ mm. (Note that the effect of truncating the iteration process is to cause the field values, expressed as a function of frequency, to be convolved with a $\sin f/f$-type curve as shown in these figures. This causes smoothing of high narrow peaks of the output function.) Fig. 8 clearly shows the resonant peaks corresponding to the quasi-TEM, the first, and the second higher order waveguide modes. Any resonant frequency corresponding to the surface mode would have appeared between the quasi-TEM and the first waveguide mode resonant frequencies (see Fig. 7). Fig. 9 shows a version of this region for 2000 iterations, but there is still no sign of a resonance corresponding to the surface or low-loss mode. Therefore we conclude that such a mode most probably does not exist.

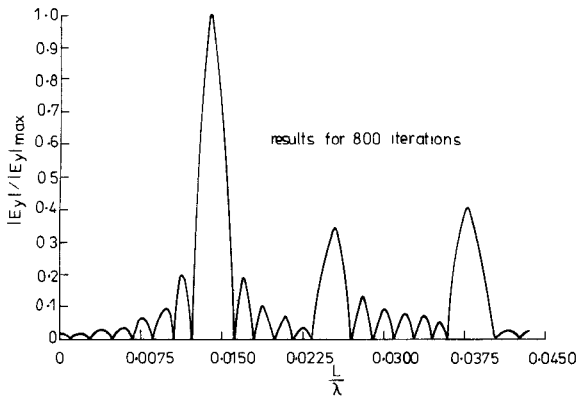

Fig. 8. A typical E-field spectrum for the resonator of Fig. 7 ($L = 3.75$ mm) clearly showing the resonant peaks corresponding to the quasi-TEM, the first, and the second waveguide modes.

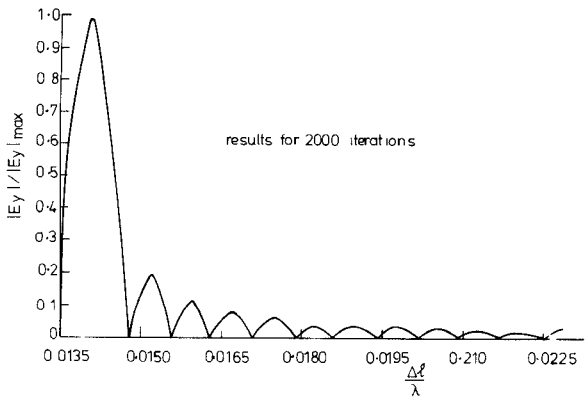

Fig. 9. A closer inspection of Fig. 8 for the range between resonant peaks of the quasi-TEM and the first waveguide mode in search of the possible existence of Daly's surface-mode resonance.

VII. SIX-COMPONENT EM FIELD DISTRIBUTIONS

With a slight modification to the general TLM program, values of the six components of EM fields at any frequency are readily available at all the nodes inside a cavity. This is considered to be important not only for the value of seeing the field distribution, but also for the following reason. In [28], the authors have shown the results for the power decay times of a number of partially filled lossy dielectric cavities. However, in all cases the initial field excitation consisted of equal amplitudes of E_y at each of the nodes and hence the decay time was not to be associated with any one particular mode. But using the field distribution information, it is proposed that the decay time for a particular mode may be found. This will be the topic of a subsequent investigation.

Figs. 10–12 show the distribution of the six electric and magnetic field components across various planes of microstrip cavity in Fig. 7. (Note that the numerical values given in Figs. 10–12 apply at the three-dimensional node cube corners as projected onto the xy plane.) The field values are for a frequency of 35.59 GHz corresponding to the dominant mode (quasi-TEM) frequency resonance of this cavity with $L = 2.25$ mm. Cross sections in the z-coordinate direction have been chosen at various distances $z = l$ from the front s/c plane of the cavity so that the particular field components in that plane will exhibit maximum values. The general characteristics of the fields are much as would be expected, i.e., the fields are mostly

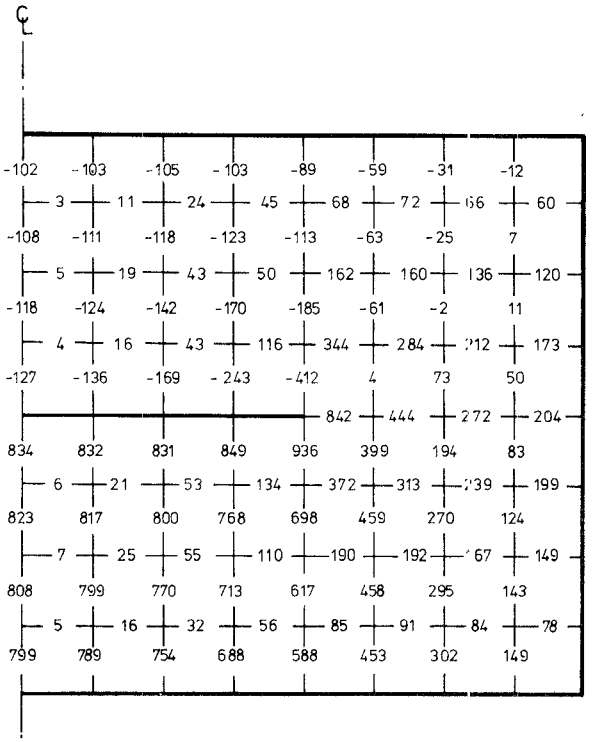

Fig. 10. Transverse electric field distribution in the x–y plane and $z = l$ for the dominant microstrip mode of Fig. 7 structure at 35.59 GHz ($L = 2.25$, $l = 1.0$ mm); horizontal number E_x, vertical number E_y.

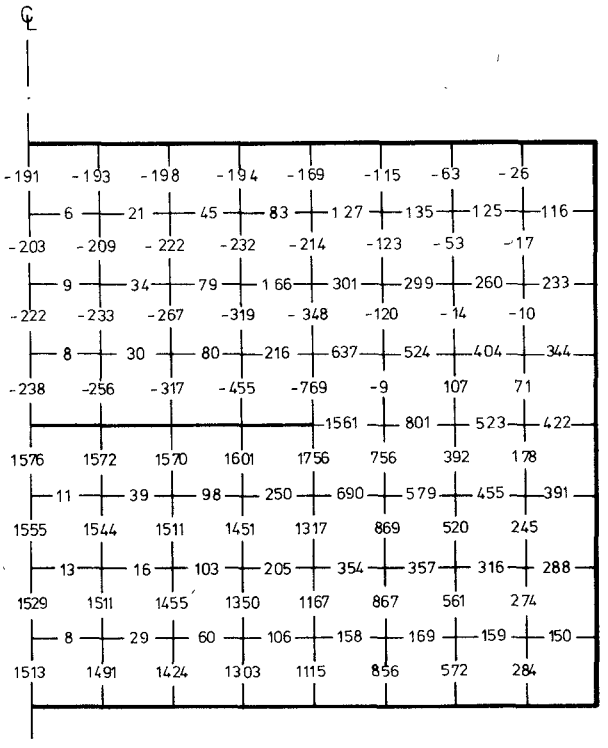

Fig. 11. Transverse magnetic field distribution in the x–y plane and $z = l$ for the dominant microstrip mode of Fig. 7 structure at 35.59 GHz ($L = 2.25$ mm, $l = 0.25$ mm); vertical number H_x, horizontal number H_y.

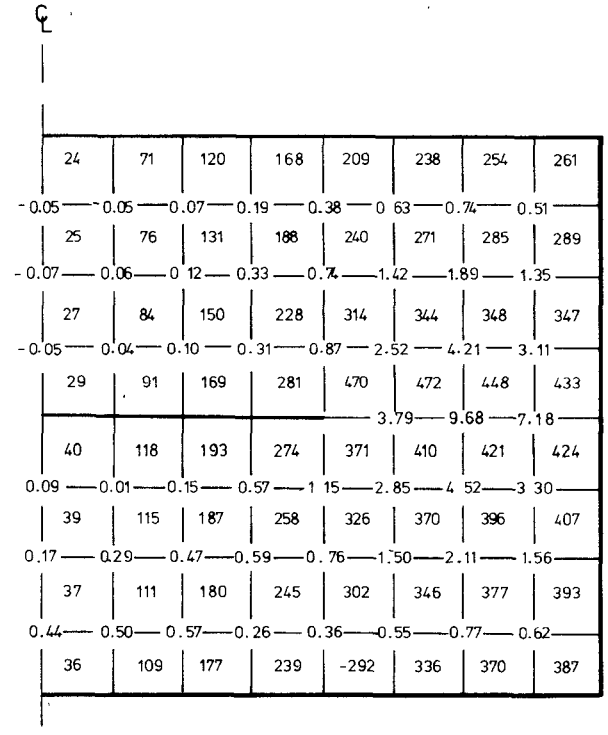

Fig. 12. Longitudinal electric and magnetic field distributions in the x–y planes with $z = l_1$ and $z = l_2$, respectively, for the dominant microstrip mode of Fig. 7 structure at 35.59 GHz ($L = 2.25$ mm, $l_1 = 0.25$ mm, $l_2 = 1.0$ mm); decimal number $-E_z$, integer number H_z.

concentrated in the dielectric, and the normal electric fields and tangential magnetic fields at or near the strip and the surrounding conductors reach a maximum.

VIII. CONCLUSIONS

This paper has demonstrated the application of the TLM method of numerical analysis to three-dimensional microstrip cavities. The main advantages of the TLM method are its ease of application, its versatility and accuracy.

The ease of application arises because of the close connection between the numerical routine and the actual physics of wave propagation [29]. For example, provided the capacitance of the lines in the TLM method are increased somehow (by using stubs in this paper) then, because all six components of the field are properly accounted for, the dielectric boundary will also be properly accounted for. Thus there is no need to introduce special numerical routines to take account of the boundary. The same argument applies to lossy materials (from zero conductivity to infinite conductivity) and hence for metallic boundaries also.

The versatility arises for similar reasons. The properties of a medium are described at each node by the two stubs, the permittivity and permeability stubs at shunt and series nodes, and the loss stub at shunt nodes. The TLM program consists, therefore, of setting the properties of the medium at each node in the first instance, and then performing the iteration process to find the way in which the fields propagate. Thus the complication of the geometry in terms of ϵ, μ, and σ is limited only to the mesh coarseness, and does not affect the program listing.

The accuracy of the method is due to the sophistication of the internodal field function which is (almost unwittingly) used when the Fourier transform is taken. In effect, the act of taking the Fourier transform puts a section of a sinusoidal function between each node. For example, in a homogeneous rectangular cavity the field functions are not solved approximately, but exactly [30]. It is for this reason that field description errors in the TLM method tend to be less than for many other methods.

However, it would be impractical to have an easily applied, versatile and accurate method if the computer running time and storage were unreasonable. While it is not possible to present formulas for the general case at this stage, it is hoped that the following figures demonstrate that the running time and storage of the TLM method are at least comparable with other methods. The first case is for the geometry of Fig. 2 for $L = 2.5$ mm using $5 \times 9 \times 6 = 270$ nodes (no symmetry properties used) and 200 iterations of the matrix. In this problem the running time was 2.16 min and the total storage was 20K words. The second example is for Fig. 5 for $2L = 5.0$ cm using $8 \times 8 \times 11 = 704$ nodes (symmetry property used) and 400 iterations. Here the time was 11.26 min using 46K words. The results are quoted for the ICL 1906A computer.

REFERENCES

[1] H. A. Wheeler, "Transmission-line properties of parallel strips separated by a dielectric sheet," *IEEE Trans. Microwave Theory Tech.*, vol. MTT-13, pp. 172–185, Mar. 1965.

[2] P. Silvester, "TEM wave properties of microstrip transmission-lines," *Proc. Inst. Elec. Eng.*, vol. 115, pp. 43–48, Jan. 1968.

[3] R. Mittra and T. Itoh, "A new technique for the analysis of the dispersion characteristics of microstrip lines," *IEEE Trans. Microwave Theory Tech.*, vol. MTT-19, pp. 47–56, Jan. 1971.

[4] J. S. Hornsby and A. Gopinath, "Numerical analysis of the dielectric-loaded waveguide with a microstrip line—Finite difference methods," *IEEE Trans. Microwave Theory Tech.*, vol. MTT-17, pp. 684–690, Sept. 1969.

[5] P. Daly, "Hybrid-mode analysis of microstrip by finite-element methods," *IEEE Trans. Microwave Theory Tech.*, vol. MTT-19, pp. 19–25, Jan. 1971.

[6] T. G. Bryant and J. A. Weiss, "Parameters of microstrip transmission lines and of coupled pairs of microstrip lines," *IEEE Trans. Microwave Theory Tech. (1968 Symp. Issue)*, vol. MTT-16, pp. 1021–1027, Dec. 1968.

[7] S. Akhtarzad, T. R. Rowbotham, and P. B. Johns, "The design of coupled microstrip lines," *IEEE Trans. Microwave Theory Tech.*, vol. MTT-23, pp. 486–492, June 1975.

[8] D. G. Corr and J. B. Davies, "Computer analysis of the fundamental and higher order modes in single and coupled microstrip," *IEEE Trans. Microwave Theory Tech.*, vol. MTT-20, pp. 669–678, Oct. 1972.

[9] R. Jansen, "Computer analysis of edge-coupled planar structures," *Electron. Lett.*, vol. 10, pp. 520–521, Nov. 1974.

[10] E. A. Mariani, C. P. Heinzman, J. P. Agrios, and S. B. Cohn, "Slot line characteristics," *IEEE Trans. Microwave Theory Tech. (1969 Symp. Issue)*, vol. MTT-17, pp. 1091–1096, Dec. 1969.

[11] C. P. Wen, "Coplanar waveguide: A surface strip transmission line suitable for nonreciprocal gyromagnetic device applications," *IEEE Trans. Microwave Theory Tech. (1969 Symp. Issue)*, vol. MTT-17, pp. 1087–1090, Dec. 1969.

[12] A. Farrar and A. T. Adams, "Matrix method for microstrip three-dimensional problems," *IEEE Trans. Microwave Theory Tech.*, vol. MTT-20, pp. 497–504, Aug. 1972.

[13] T. Itoh, "Analysis of microstrip resonators," *IEEE Trans. Microwave Theory Tech.*, vol. MTT-22, pp. 946–952, Nov. 1974.

[14] R. Jansen, "Shielded rectangular microstrip disc resonators," *Electron. Lett.*, vol. 10, pp. 299–300, July 1974.

[15] S. Akhtarzad, "Analysis of lossy microwave structures and microstrip resonators by the TLM method," Ph.D. dissertation, Univ. Nottingham, Nottingham, England, May 1975.

[16] S. Akhtarzad and P. B. Johns, "The dispersion characteristic of a microstrip line with a step discontinuity," *Electron. Lett.*, vol. 11, pp. 310–311, July 1975.

[17] ——, "Transmission-line matrix solution of waveguides with dielectric losses," *Int. J. Numer. Meth. Eng.*, vol. 9, 1975.

[18] P. B. Johns, "The solution of inhomogeneous waveguide problems using a transmission-line matrix," *IEEE Trans. Microwave Theory Tech. (Special Issue on Computer-Oriented Microwave Practices)*, vol. MTT-22, pp. 209–215, Mar. 1974.

[19] S. Akhtarzad and P. B. Johns, "The transmission-line matrix solution of waveguides with wall losses," *Electron. Lett.*, vol. 9, pp. 335–336, July 1973.

[20] ——, "Numerical solution of lossy waveguides—TLM computer program," *Electron. Lett.*, vol. 10, pp. 309–311, July 1974.

[21] T. Itoh and R. Mittra, "A technique for computer dispersion characteristics of shielded microstrip lines with the application to the junction problems," in *Proc. 4th European Microwave Conf.* (Montreux, Switzerland), Sept. 10–13, 1975, pp. 373–377.

[22] R. A. Pucel and D. J. Massé, "Microstrip propagation on magnetic substrates—Part I: Design theory," *IEEE Trans. Microwave Theory Tech.*, vol. MTT-20, pp. 304–308, May 1972.

[23] S. Akhtarzad and P. B. Johns, "TLM analysis of the dispersion characteristics of microstrip lines on magnetic substrates using three-dimensional resonators," *Electron. Lett.*, vol. 11, pp. 130–131, Mar. 1975.

[24] R. A. Pucel and D. J. Massé, "Microstrip propagation on magnetic substrates—Part II: Experiment," *IEEE Trans. Microwave Theory Tech.*, vol. MTT-20, pp. 309–313, May 1972.

[25] O. C. Zienkiewitz and Y. K. Cheung, *The Finite-Element Method in Structural and Continuum Mechanics.* New York: McGraw-Hill, 1967.

[26] R. E. Collin, *Field Theory of Guided Waves.* New York: McGraw-Hill, 1960.

[27] C. G. Williams and G. K. Cambrell, "Numerical solution of surface waveguide modes using transverse field components," *IEEE Trans. Microwave Theory Tech.* (Short Papers), vol. MTT-22, pp. 329–330, Mar. 1974.

[28] S. Akhtarzad and P. B. Johns, "The solution of 6-component electromagnetic fields in three space dimensions and time by the TLM method," *Electron. Lett.*, vol. 10, pp. 535–537, Dec. 1974.

[29] P. B. Johns, "A new mathematical model," *Radio Electron. Eng.*, vol. 44, pp. 657–666, Dec. 1974.

[30] P. B. Johns, "Application of the transmission-line matrix method to homogeneous waveguides of arbitrary cross-section," *Proc. Inst. Elec. Eng.*, vol. 119, pp. 1086–1091, Aug. 1972.

[31] S. Akhtarzad and P. B. Johns, "Generalized elements for the TLM method of numerical analysis," *Proc. Inst. Elec. Eng.*, vol. 122, Dec. 1975.

[32] ——, "The solution of Maxwell's equations in three space dimensions and time by the TLM method on numerical analysis," *Proc. Inst. Elec. Eng.*, vol. 122, Dec. 1975.